SiliconPV 2024, 14th International Conference on Crystalline Silicon Photovoltaics
Silicon Material and Defect Engineering
https://doi.org/10.52825/siliconpv.v2i.1284

Published: 06 Dec. 2024

Inline Measurement of Light Beam Induced Current (LBIC) Under High-Injection and Reverse Bias Conditions

Marko Turek[1], Yuriy Tymyrivskyy[1], Stephan Hensel[1], and Manuel Meusel[1]

[1]Fraunhofer IMWS, Germany

*Correspondence: Marko Turek, marko.turek@csp.fraunhofer.de

Abstract. Quality control in solar cell production relies on characterization methods that are fast enough to yield information on the properties of each solar cell in less than about one second. Imaging techniques such as electroluminescence (EL) are well established methods revealing spatially resolved quality mappings. Scanning techniques such as light beam induced current (LBIC) are common laboratory methods yielding complementary information but do not meet the speed requirements. In our work, we analyse an inline implementation of the LBIC method which is extended with respect to its measurement parameters, i.e., both the laser power and a solar cell bias-voltage are varied. As these extended conditions differ from conventional LBIC-applications at zero bias and low injection, we compare our inline-LBIC images with EL images and conventional LBIC images by means of an image contrast analysis. We find that our method resembles more the EL imaging as variations in the local series resistance are prominently detected. Thus, the proposed LBIC approach with extended measurement parameter range can yield both local short circuit information and local series resistance information. With our setup, measurement speeds around 700 ms are achieved.

Keywords: Solar Cells, Metrology, Light Beam Induced Current LBIC

1. Introduction and Motivation

The throughput in solar cell production lines continuously increases while the solar cell technologies become more complex at the same time. This requires new and fast characterization approaches targeting at a fully automated in-line quality control system. On the one side, there are several new developments related to spectrally resolved current-voltage-measurements, like rapid-EQE approaches [1], or more advanced series resistance measurements, e.g. described in [2], using LED sun simulators. On the other side, the identification of lateral non-uniformities plays a major role besides the determination of full-cell performance parameters that can be deduced from current-voltage measurements. Here, electroluminescence imaging is a standard method in many solar cell production lines.

However, there are also other approaches which are commonly applied off-line to a reduced number of cells in characterization laboratories as they do not meet the requirements regarding their data acquisition times. For example, a high-resolution LBIC measurement can take several seconds up to minutes in a conventional lab tool. On the other hand, additional complementary information on the solar cell's quality can be obtained from these scanning techniques, for example information on local currents for various excitation wavelengths.

EL-imaging requires a bias voltage and reveals cell defects and series resistance effects such as cracks or finger interruption. Conventional LBIC imaging at zero bias and low currents induced by the light spot is less sensitive to local series resistance as it measures the locally induced short circuit current. However, depth-sensitive information can be obtained by implementing several distinct LBIC wavelengths which results in an effective local quantum efficiency measurement. In a typical lab-LBIC-setup, the measurement times are not sufficient for an inline implementation but there have been various approaches to increase measurement speed, e.g. presented in [3], [4]. Also, more advanced LBIC techniques which also modify the cell's voltage have been studied intensively [5].

With increasing automation and digitalization of production lines together with increasingly better image analysis software using neural networks, a quantitative assessment of imaging in correlation to performance parameters comes more and more into focus [6], [7]. Thus, more complex cell architectures, like tandem cells, will require a broader range of metrology and imaging included into the production lines. In our work, we present a measurement parameter analysis of an inline LBIC setup. To this end, a laser source with a laser-scanner unit has been integrated into a fully automated lab-to-fab test platform for characterization tests under inline conditions. In parallel, all test cells were characterized using EL-imaging and conventional lab-LBIC-scans at multiple wavelengths. We find that our implemented inline-LBIC resembles more the EL-imaging than the LBIC-scan under certain measurement parameter conditions. In particular, we applied a specific high-injection together with a reverse biasing of the solar cells during measurement.

For a more quantitative understanding of these differences between conventional lab-LBIC at zero bias and low injection and our inline-LBIC with reverse bias and high injection, a numerical model based on electrical circuits has been setup to analyze trends in imaging contrasts related to local cell parameter variations. Using this numerical model, a systematic parameter study on the impact of the measurement conditions, e.g. laser-induced carrier injection and cell bias-voltage, on the local imaging contrasts is presented. Thus, this model allows a systematic improvement of the required measurement parameters for certain cell types or applications.

2. Experimental Approach and Data Analysis

An inline-LBIC setup has been integrated into a fully automated lab-to-fab test platform achieving measurement times around 700 ms. It features a laser source combined with a laser scanner. Furthermore, a measurement electronics acquires the cell's time-resolved current leading to an image of the entire solar cell. Another current source is employed to apply a bias voltage to the solar cell during measurement. It is important to note, that in our case the inline-LBIC measurement is performed under high-injection conditions, i.e., the measured local cell currents are in a range of several mA for a sub-mm laser spot.

To analyze the resulting inline-LBIC images, test cells with specific defects have been prepared by laser processing the solar cell's surfaces, see Figure 1. In particular, we have investigated intrinsic cell defects (the right side of the cell labelled with no. 1 in Figure 1), and artificially induced laser-scribe line defects (no. 2 and no 3.). In a first step, the cells have been characterized using conventional lab-LBIC-scans, EL-imaging, and then by our inline-LBIC.

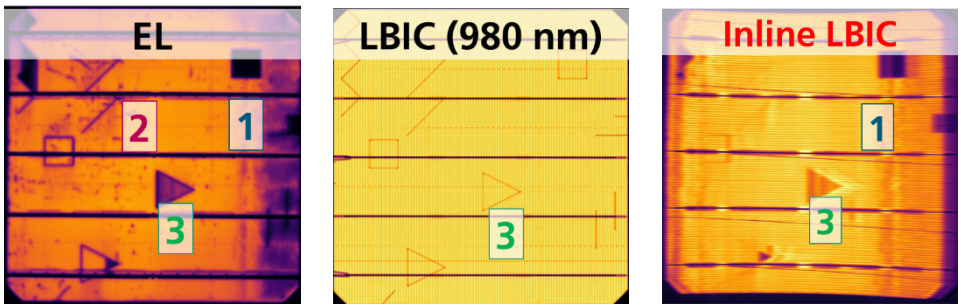

Figure 1. *Imaging of a solar cell with different types of line defects and two-dimensional defects: (left) EL-imaging, (center) conventional LBIC-scan at 980nm, (right) inline-LBIC at high injection and reverse bias.*

From the EL-image, it is evident, that the intrinsic cell defect as well as the laser-induced line defects are detected with high contrast. It is important to note that the defect type no. 3 is caused by a line forming a closed loop. In this way, the fingers that circumvent the triangular region no. 3 in Figure 1, are thinned so that this region is (partially) isolated. This corresponds to an increased local series resistance within the triangle and leads to the high contrast in the EL-image. Although a similar laser process has been applied to the square-shape region on the left side, its inner part is still connected to the bus bar thus connecting it to the current source during EL-imaging. Hence, this squared shaped part is not related to an increase series resistance by finger thinning and therefor appears bright in the EL-image. This interpretation, that the triangular shape no. 3 is characterized by an increased local series resistance due to finger thinning is support by the LBIC-image. LBIC imaging gives information on the local short circuit currents which are rather insensitive to series effects. Therefore, the laser lines are clearly visible while the inner part of the triangle does not show an increased contrast.

To achieve a quantitative analysis of the trends observed in the measurements, a trend analysis of the image contrasts of several defects compared to a defect-free part of the solar cell has been performed. For example, the signal strength of the triangular defect in the cell center, marked by no.3 in Figure 1, is compared to an intact cell region right next to the defect in dependence of the applied laser intensity and cell bias voltage. This contrast analysis has been applied to the same cell measured with our inline-LBIC under varying measurement conditions.

Finally, a numerical model was developed that can describe the observed trends in the measured contrasts. It includes an electrical equivalent circuit based on a two-diode-setup with an extension for the reverse characteristics following the Bishop model [8]. The model has been implemented in Python using an in-house solar cell simulation library that can simulate the current-voltage-curve of any parallel or series connection of an arbitrary number of solar cells. Furthermore, additional electrical components like an external series resistance describing the contacting of the measurement setup are also included and can be adapted according to the experimental conditions. To simulate the biased LBIC-measurement, the locally illuminated part is numerically calculated separately from the remaining dark part of the cell to obtain the combined current-voltage curve. Using this model, a variation of the local cell parameters has been performed. This approach allows for an analysis of the impact of the measurement conditions on the imaging contrasts caused by local variations of cell properties thus allowing for an optimization of the measurement process.

3. Results

When our inline-LBIC with extended measurement parameters, i.e. bias-voltage and higher injection, is compared to the EL-image and lab-LBIC-image, it becomes evident, that the series resistance effects also become visible in this measurement configuration, see Figure 1. Fur-

thermore, some shadow-like wave-effects are visible in particular near the cell edges. However, these are related to the high measurement speeds and will be compensated by upcoming hardware and software improvements of the current setup. In the next step, we collected all the data obtained by variation of either the light intensity or the bias voltage, see Figure 2.

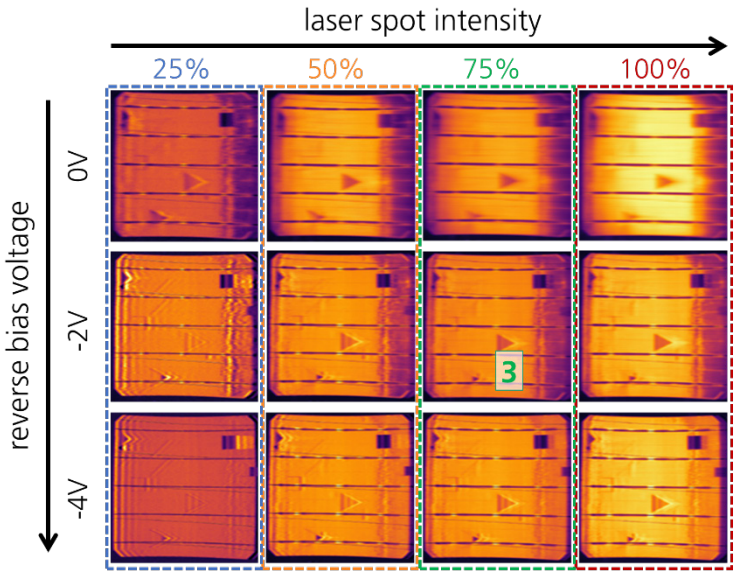

Figure 2. *Resulting inline-LBIC images with variation in laser spot intensity and reverse bias voltage.*

We find that there are very pronounced changes in imaging contrast of our inline-LBIC when the measurement parameters, i.e., laser power (carrier injection) and reverse cell bias voltages, are modified. Lower laser powers generally lead to less contrasts between the singal in a defect region and the signal of the unaffected cell parts. This is even more so if the bias voltage is increased, see Figure 2. A quantitative summary of these findings for the contrasts of the triangular defect marked with no. 3 as the region of interest ROI compared to an average cell region right next to it is shown in Figure 3 (left). To obtain these trends in contrast from the LBIC images, the local LBIC-signal is averaged over a representative area next to the ROI and compared to the signal within the ROI, i.e. triangle no. 3, itself. If these two parts exhibit similar signals, then the relative contrast of the defect is close to 0% and the defect is barely observable. On the other hand, if the signal within the ROI and next to the ROI is very different, i.e. when the ROI appears much darker, then the relative contrast of the ROI compared to its surrounding is significantly larger than 0%.

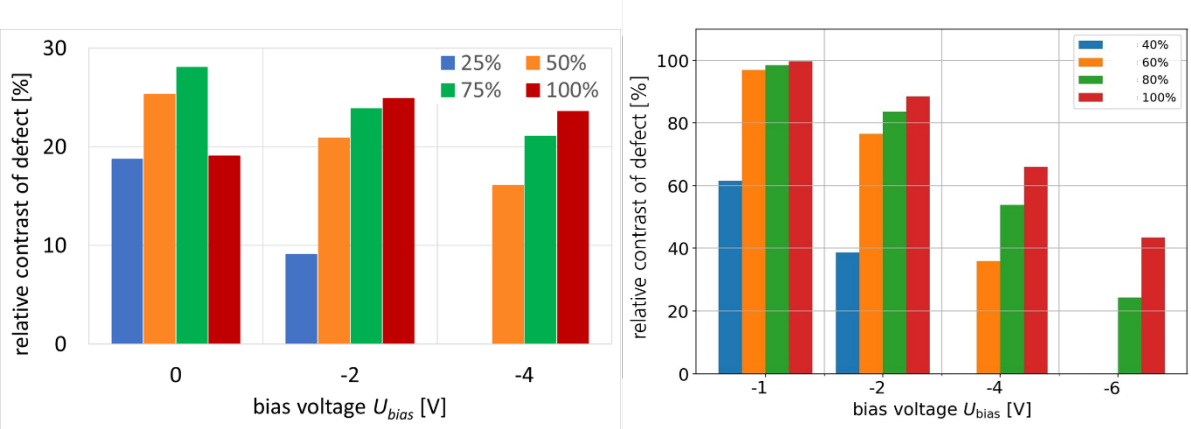

Figure 3. *(left) Contrast analysis of the triangular region (labelled no. 3 in Figure 1) for variations of bias voltage and laser power. (right) Same quantity obtained from the simulation model.*

Several trends can be observed for the changes in contrast with variations in measurement parameters. Higher intensities (laser power) at fixed bias voltages are related to higher contrasts, e.g. increasing the laser power 25% → 50% → 75% → 100% at U_{bias} = -2V. This effect shows some saturation or even a decrease as for U_{bias} = 0V. For fixed laser intensities, e.g. 50% represented by the orange bars, the contrast decreases with higher values of reverse bias, e.g. going from 0V → -2V → -4V. For lower laser powers, this might even lead to a vanishing contrast as observed for 25% laser power and -4V bias voltage.

The simulation model, we have developed, exhibits very similar trends, see Figure 3 (right). Again, fixed bias voltage with increasing laser power implies an increase in contrast which saturates at higher laser powers. On the other hand, increasing the value of the reverse bias while keeping the laser power fixed implies a reduction in contrast and can lead to complete loss of contrast. Thus, our model represents the underlying mechanisms during the inline-LBIC measurement rather well as it describes the general trends. In particular, it shows that a local series resistance variation leads to a signal contrast which is not observed for conventional lab-LBIC at zero bias and low injection. However, a quantitative modelling of the absolute current values would require further improvements. In particular, the laser spot size, its intensity and the local series resistance variations need to be included in a more quantified manner by determination of their exact values under the given experimental conditions. Nevertheless, already at this stage, our model can serve as a guideline to further optimize the measurement process as it describes all major trends.

4. Summary and Conclusions

In our work, we present an inline-LBIC method with extended measurement parameter range. In particular, we show that applying a bias voltage and increasing the laser spot intensity reveals local information on the series resistance rather than the short current density as obtained in lab-LBIC setups with zero bias and low intensities. Additionally, our setup has been integrated into a fully automated lab-to-fab platform demonstrating its potential for an inline application. Furthermore, the experimental setup is supplement by implementation of a numerical model, which describes all major trends of the measurement signal related to the variation of measurement conditions very well on a qualitative level.

These results are of particular interest as they would allow for a mapping of two major quantities, i.e. local short circuit current and local series resistance effects, by the same hardware setup when the measurement parameters are changed. Thus, it could yield similar information as EL-imaging, i.e. series resistance imaging, but also additional information given by the local short circuit current. This would allow for a much improved laterally resolved loss analysis going beyond EL-imaging which will be of particular interest in upcoming tandem solar cell technologies. As a single measurement can be realized in several hundreds of milliseconds, this approach is suitable for inline-application.

Data availability statement

Measurement data can be provided by the authors upon request.

Author contributions

Marko Turek has contributed to this work regarding conceptualization, data curation, formal analysis, methodology, software development, funding acquisition, supervision and writing. Yuriy Tymyrivskyy has contributed by data curation, formal analysis, methodology and software development. Stephan Hensel and Manuel Meusel have contributed by conducting experiments and data acquisition, providing resources and samples.

Competing interests

The authors declare that they have no competing interests.

Funding

This work has received funding by the German federal ministry for Economic Affairs and Climate Action as it has been conducted within the “OptiLearn” project (FKZ 03EE1108A).

References

[1] M Turek, K Sporleder, T Luka, *Spectral characterization of solar cells and modules using LED-based solar simulators*, Solar energy materials and solar cells 194, 142-147 (2019), doi: https://doi.org/10.1016/j.solmat.2019.02.007.

[2] M Turek, *Current and illumination dependent series resistance of solar cells*, Journal of applied physics 115, 14 (2014), doi: https://doi.org/10.1063/1.4871017.

[3] M. Acciarri, S. Binetti, A. Racz, S. Pizzini, G. Agostinelli, *Fast LBIC in-line characterization for process quality control in the photovoltaic industry*, Solar Energy Materials and Solar Cells 72, 417-424 (2002), doi: https://doi.org/10.1016/S0927-0248(01)00189-1.

[4] G. Koutsourakis, M. Cashmore, S.R.G. Hall, M. Bliss, T.R. Betts, R. Gottschalg, *Compressed Sensing Current Mapping Spatial Characterization of Photovoltaic Devices*, IEEE Journal of Photovoltaics 7, 486 (2017), doi: https://doi.org/10.1109/JPHOTOV.2016.2646900.

[5] J Carstensen, G Popkirov, J Bahr, H. Föll, *CELLO: an advanced LBIC measurement technique for solar cell local characterization*, Solar Energy Materials & Solar Cells 76, 599–611 (2003), doi: https://doi.org/10.1016/S0927-0248(02)00270-2.

[6] M Turek, M Meusel, *Automated classification of electroluminescence images using artificial neural networks in correlation to solar cell performance parameters*, Solar Energy Materials and Solar Cells 260, 112483 (2023), doi: https://doi.org/10.1016/j.solmat.2023.112483.

[7] M. Alt, S. Fischer, S. Schenk, S. Zimmermann, K. Ramspeck, M. Meixner, *Electroluminescence imaging and automatic cell classification in mass production of silicon solar cells*, IEEE 7th World Conference on Photovoltaic Energy Conversion, Wcpec, pp. 3298-3304 (2018), doi: https://doi.org/10.1109/PVSC.2018.8547983.

[8] Bishop, J. Computer simulation of the effects of electrical mismatches in photovoltaic cell interconnection circuits. Sol. Cells 25, 73–89 (1988), doi: https://doi.org/10.1016/0379-6787(88)90059-2.